High-Pressure Synthesis and Structural Behavior of Sodium Orthonitrate Na_3NO_4

R. Quesada Cabrera[a], A. Sella[a], E. Bailey[a], O. Leynaud[a,b] , P.F. McMillan[a,*]

[a]*Department of Chemistry and Materials Chemistry Centre, Christopher Ingold Laboratories, University College London, 20 Gordon Street, London WC1H 0AJ, United Kingdom*
[b]*Institut Néel, CNRS, 25 rue des Martyrs, Grenoble, France*

*Corresponding author. Fax:+442076797463.
E-mail address: p.f.mcmillan@ucl.ac.uk (P.F.McMillan).

Abstract

Sodium orthonitrate (Na_3NO_4) is an unusual phase containing isolated NO_4^{3-} groups. Previous syntheses were obtained by heating $NaNO_3$ and Na_2O for extended periods (>14 days) in evacuated chambers. Now we show that the phase can be prepared rapidly from mixtures of the precursors at high pressure consistent with the negative volume change between reactants and products. The high-pressure behavior of Na_3NO_4 was studied using Raman spectroscopy and synchrotron X-ray diffraction in a diamond anvil cell above 60 GPa. We found no evidence for major structural transformations indicating the structural stability of NO_4^{3-} ions, even following laser heating experiments carried out at high pressure, although broadening of Raman peaks could indicate the onset of disordering at higher pressure.

Keywords

Sodium orthonitrate; sodium oxide; sodium nitrate; high-pressure synthesis; diamond anvil cell; pressure-induced amorphization.

1. Introduction

Structures based on tetrahedrally-bonded oxoanions form a range of important minerals and materials including sulfates, phosphates and especially the orthosilicates, containing isolated $SiO_4^{4-,}$ groups that are major components of the Earth's upper mantle. Such silicate anions are well known to polymerize to form chains, sheets, and three-dimensional network structures. The high-pressure behavior of these tetrahedrally coordinated species has been studied extensively because of density-driven transitions to higher coordinated structures that are important for mantle mineralogy. For example, $(Mg, Fe)_2SiO_4$ olivines transform to spinel structures containing silicon in octahedral coordination and this marks

the passage between the upper and lower mantle within the Earth. Octahedrally coordinated silicon also occurs in other high-pressure mantle minerals including silicate perovskite, ilmenite, and garnet structures and SiO_2 polymorph stishovite [1]. Unusual five-fold coordinated silicate species have been identified in glasses prepared at high pressure and these play an important role in the densification and viscous flow of the molten materials [2]. Compression of $(Mg,Fe)_2SiO_4$ crystals and glasses at low temperature was suggested to result in formation of such highly-coordinated species and linkages between the orthosilicate anions at pressures near 50 GPa [3].

It is notable that tetrahedral oxoanion species are generally formed with atoms of the second and higher rows of the periodic table (Si, P, S, Cl, Ge, As etc). By contrast, the first row elements tend to form trigonal species (BO_3^{3-}, CO_3^{2-}, NO_3^-). However, a tetrahedral oxoanion chemistry does occur for boron, either co-polymerized with other species or as isolated $B(OH)_4^-$ anions (e.g., in $LiB(OH)_4$). A long-standing question has been whether structures based on tetrahedral NO_4^{3-} or CO_4^{4-} units can be prepared, and what the extent of their thermodynamic or kinetic stability might be. The occurrence of tetrahedral orthocarbonate species would have implications for carbon storage within mineral or melt species deep within the Earth [4], as well as for developing the solid state chemistry of these "light element" species [5-10].

Ionic orthocarbonate species containing CO_4^{4-} groups have not yet been synthesized but *ab initio* calculations and molar volume considerations indicate that they might form at high pressure [8-10]. Tetrahedrally bonded structures containing polymerized CO_4 groups analogous to the SiO_2 polymorphs have been obtained by high-P,T treatment of CO_2 [11]. *Ab initio* calculations have suggested that MCO_3 (M= Sr, Ca) minerals can transform into polymeric chain structures containing linked CO_4 tetrahedra at pressures extending into the megabar range, and this is borne out by experiments [12]. Recent high-pressure studies on CO_2 have indicated formation of glassy "carbonia" that might contain even higher-coordinated (5- or 6-coordinated) carbonate species [13].

The intrinsic stability of tetrahedral clusters with central atoms within the first row of the periodic table has been established by *ab initio* calculations [14]. A first example of a solid-state orthonitrate structure was synthesised by Jansen [5], who obtained Na_3NO_4 containing isolated NO_4^{3-} units by reaction of Na_2O with $NaNO_3$, as well as K_3NO_4 by a similar method (Fig. 1). The nature of the compound was first established by Raman spectroscopy in 1977 [6] and a structural analysis based on single crystals grown over a long time period (up to 240 days) was reported subsequently [7]. The ambient pressure

synthesis of the orthonitrate phase normally requires heating for prolonged periods ranging from weeks to days. However, taking advantage of the negative volume change between reactants and products it is possible to accelerate the synthesis reaction. We tested that prediction by synthesis experiments in a multi-anvil device. Furthermore, we investigated the high-pressure behavior of Na_3NO_4 and stability of the NO_4^{3-} units above 60 GPa using synchrotron X-ray diffraction and Raman spectroscopy in the diamond anvil cell (DAC). We also carried out laser heating experiments under high pressure conditions to examine the stability of the orthonitrate structure.

2. Experimental

We first obtained Na_3NO_4 samples for high-pressure experiments by reaction between Na_2O and $NaNO_3$ at ambient pressure, following the synthesis method reported originally by Jansen [5]. Reactants (Na_2O 80%, $NaNO_3$ 99.9%) were obtained from *Aldrich* and used as delivered. The Na_2O material also contained Na_2O_2 as an impurity phase, but this was not considered an impediment to the synthesis reaction. The starting materials were stored and handled in a dry box (N_2 atmosphere; <10 ppm O_2/H_2O). The Na_2O and $NaNO_3$ powders were ground together in an approximately 3:1 ratio and loaded into Ag capsules that were crimped shut, transferred to a glass tube and sealed under vacuum before heating at 380 ºC (10 $^{\circ}C\ h^{-1}$) for 14-90 days.

The diamond anvil cell (DAC) experiments were carried out using 4-post screw-driven cells with diamond anvil culet diameters ranging between 150 and 300 μm. Pre-indented Re gaskets were drilled with 80-μm diameter holes. Ruby chips were added to determine the pressure inside the sample chamber [15]. Raman spectroscopy was carried using a home-built system based on Kaiser supernotch filters, Acton spectrograph and LN_2 cooled back-thinned CCD detector [16]. An Ar^+ laser (514.5 nm, ~1 mW) was focused onto the sample using a 50x Mitutoyo objective and Raman data were collected using backscattering geometry. The *in situ* high-pressure Raman and synchrotron X-ray diffraction experiments were carried out using Na_3NO_4 samples loaded inside the glove box without any pressure-transmitting medium to avoid potential reactions with air/moisture. The resulting experiments were carried out under non-hydrostatic conditions that will slightly affect the compressional parameters but would promote phase transformations and structural changes at high pressure, that were the main focus of our study. The presence of some unreacted Na2O within the sample mixture also provided an

opportunity to measure the compressional behavior of this anti-fluorite structured compound. For laser heating experiments, we used a CO_2 laser (λ=10.6 μm; 75 W), focused inside the sample area and relying on the surrounding material that is a wide-gap insulating material with low thermal conductivity to avoid excessive heat transfer to the diamonds.

The samples at ambient pressure were characterized by powder X-ray diffraction in sealed capillaries using a Stoe StadiP diffractometer and Cu K_{α} radiation (λ= 1.5402 Å) and by Raman spectroscopy. For *in situ* X-ray diffraction experiments, angle-dispersive X-ray diffraction data were first obtained at station 9.5 HPHT, Daresbury SRS using λ= 0.444 Å. This facility is no longer in existence but has had a long career of pioneering *in situ* synchrotron experiments, including high-P,T studies and for new materials synthesis [17]. The X-ray beam was collimated and focused to 30 μm inside the cell using newly developed Laue optics at the station [18]. Further data were obtained at ESRF BM01A (Swiss-Norwegian beam lines) using angle-dispersive techniques (λ = 0.700 Å). The resulting two-dimensional X-ray patterns were integrated and converted to 1D intensity versus 2Θ or d-value plots using Fit2D [19]. The structures were refined by the Ritevled method using FULLPROF [20].

3. Results and Discussion

3.1. Synthesis of Na_3NO_4 from Na_2O + $NaNO_3$ at ambient vs high pressure

Initial traces of Na_3NO_4 formed after reaction between intimately mixed Na_2O (+Na_2O_2 present as an impurity in the starting sample) and $NaNO_3$ at 380°C at ambient pressure was detected after 7-14 days [5-7]. We achieved synthesis of nearly pure Na_3NO_4 samples at ambient pressure only after 90 days, comparable with the time sale required in the original study using highly purified starting materials to produce Na_3NO_4 single crystals (240 days) [5]. It is worth noting that these reaction times may be affected by the purity of the precursors and that commercial Na_2O with 80% purity was used in our experiments, instead of the pure Na_2O used in the original work reported in ref. [5]. Examination of the molar volumes of reactants and products involved in the synthesis reaction $Na_2O + NaNO_3 \rightarrow Na_3NO_4$ (i.e., V_{Na3NO4}= 57.20 cm^3 mol^{-1}, V_{Na2O}= 27.31 cm^3 mol^{-1} and V_{NaNO3}= 36.95 cm^3 mol^{-1}) indicates a negative reaction volume of $\Delta V = -7.06$ cm^3 mol^{-1}, suggesting that

formation of the orthonitrate is favored at high pressure. This is confirmed by multi-anvil synthesis experiments, in which Na_3NO_4 formation was observed after only 2 days treatment at 4 GPa and 500˚C. The high-pressure synthesis was carried out using a 1,000-ton Walker-type multianvil press [21]. The $Na_2O/NaNO_3$ precursor mixture was prepared as described in the experimental section, sealed in a Pt capsule (~5 mm^3) inside the glove box and loaded into an octahedral assembly formed by crushable ceramic (MgO-based mixtures) and a graphite furnace, with W/Re thermocouples used for temperature measurement and control. After pressurization at 4 GPa, the mixture was heated up to 500 ºC (10 ˚C h^{-1}) and held for 50 h before quenching by turning off the furnace power. After both ambient and hgh-P,T reactions, phases present in our samples included some unreacted Na_2O, $NaNO_3$ with occasionally Na_2O_2, that were detectable by Raman spectroscopy.

The X-ray diffraction (XRD) patterns obtained from both the ambient-pressure and high-pressure syntheses are compared with those of the reported Na_3NO_4 structure [5] and the precursor mixture in Fig. 2. We confirmed that the main phase obtained by the ambient-pressure method (Fig.2(c)) was Na_3NO_4 (~98% in weight), Na_2O and $NaNO_3$ being present as minor impurities (~0.4% and 1.1%, respectively). Refinement of the structure synthesized at ambient pressure indicated that the unit cell parameters a= 8.631(7) Å, b= 9.729(8) Å and c= 9.04251 Å are close to literature values [5]. We noted that the diffraction peaks are slightly split in this pattern, indicating inhomogeneity of the sample. However, lower symmetry can be rejected on the basis of Miller indices of the split reflections.

The Raman spectrum of Na_3NO_4 at room conditions is dominated by a strong peak at 843 cm^{-1} (υ_1) due to symmetric NO_4^{3-} stretching vibrations. The antisymmetric N–O stretching vibrations that are plit into individual components by the site group symmetry as well as by interactions between NO_4^{3-} species within the unit cell occur at ~1000 cm^{-1} (υ_3). Symmetric and antisymmetric O–N–O bending modes appear between 650 and 670 cm^{-1} (υ_4) and at 540 cm^{-1} (υ_2), respectively [5]. The Raman studies also demonstrated the presence of some unreacted Na_2O and $NaNO_3$ within the samples, via stringly Raman active features that are present even at very low concentrations. The band at 240 cm^{-1} corresponds to the triply degenerate stretching mode of Na_2O, whereas the band at 1058 cm^{-1} along with a shoulder at 1067 cm^{-1} are due to the NO_3 stretching vibrations of $NaNO_3$ (**Error! Reference source not found.**).

3.2. Raman spectroscopy at high pressure

The high-pressure structural behavior of Na_3NO_4 was investigated using Raman spectroscopy up to 61 GPa (**Error! Reference source not found.**). The micro-Raman technique (3-4 μm) allowed recording spectra of Na_3NO_4 alone, avoiding interference of Na_2O or $NaNO_3$ vibrational bands. No major changes were recorded in the Na_3NO_4 spectrum obtained at high pressure, indicating that the orthonitrate structure is highly resistant to change upon compression within this range. The appearance of a new peak within the manifold of υ_4 bending modes above 21 GPa (Fig. 5) suggests a change in crystal packing or local symmetry of the NO_4^{3-} groups within this pressure range. Compression beyond 40 GPa results in the appearance of additional weak spectral features in the region between 300-450 cm^{-1} suggesting additional crystal structure changes. However, these results only indicate minor structural rearrangements that may occur within the Na_3NO_4 lattice at high pressures, and all the spectral changes are fully reversible during decompression to ambient conditions at room temperature (Fig. 5).

3.3. Synchrotron X-ray diffraction at high pressure

X-ray diffraction patterns of the reaction components recorded upon compression are shown in Fig. 6. Some peak broadening occurred due to the non-hydrostatic conditions. The X-ray diffraction experiments sampled a much larger volume of the material within the DAC compared to the microbeam Raman results described above. The X-ray beam at SRS 9.5HPHT could be collimated/focused to ~30 μm and the diameter of the DAC gasket hole was ~80 μm, so features from Na_2O and $NaNO_3$ were always present along with the Na_3NO_4 reflections, and these had to be accounted for during the data analysis.

There were no significant changes observed in the X-ray diffraction patterns up to 10 GPa (Fig. 6). Above 10 GPa, all reflections associated with Na_2O broadened and vanished while a broad signal was observed at $2\theta \sim 13.5^{\circ}$. The $NaNO_3$ features also seem to undergo dramatic peak broadening and intensity decrease. A minor rearrangement of the $NaNO_3$ compound occurs at above 13 GPa, indicated by the changes observed in the 11-13° region of the X-ray diffraction patterns (Fig. 6). This is consistent with our Raman results (Fig. 5). Attempts to analyze the high-pressure Na_3NO_4 structure using Rietveld methods were unsiccessful. Beyond 25 GPa, the diffraction patterns are dominated by the

broad peak due to an amorphous components. However, diffraction peaks from the crystalline Na_3NO_4 phase are still present up to 64 GPa.

We could follow the variation of unit cell parameters and volume up to 25 GPa (Fig. 7). The bulk modulus of Na_3NO_4 (K_0=43 GPa, assuming K_0'=4) was estimated using a Birch-Murnaghan fit. This is comparable to values predicted for orthocarbonate phases (e.g., Li4CO4: 46 GPa, Ref [10]) and compounds such as sodium oxide nitrite (47.5 GPa) [22] or nitrosonium nitrate (45.2 GPa) [23].

The bulk modulus of Na_2O has not yet been reported in the literature. The modulus of Na_2O estimated from our data was K_o= 83 GPa assuming K_0'=4, comparable with that for Li_2O but significantly larger than predicted values for K_2O or Rb_2O [24] (Table 1).

3.4. Laser heating of Na_3NO_4 at high pressure

A laser-heating experiment was carried out for the exploration of new possible high-pressure polymorphs of Na_3NO_4. The sample does not absorb the λ~1μm radiation but ruby chips added to the sample for pressure determination acted as internal heaters. This method did not allow a reliable estimation of the temperature in the sample. We performed the heating experiments using similar conditions that led to the synthesis of polymeric CO_2-V (40 GPa, ~2000K) [11] in our laboratory (Fig. 8, inset). The Raman spectrum of Na_3NO_4 before heating is shown in Fig. 8(A). After laser heating, the pressure dropped to 36 GPa. Raman spectra were collected from different areas in the sample. Raman spectra recorded from different areas in the sample did not seem to indicate any substantial change in the structure of Na_3NO_4 (Fig. 8). However, a broad feature at 350-480 cm^{-1} might indicate the formation of amorphous Na_xNO_y materials..

4. Conclusion

The high pressure synthesis of sodium orthonitrate (Na_3NO_4) from Na_2O and $NaNO_3$ resulted in a NO_4^{3-}-containing polymorph of undetermined structure. The slow temperature ramp and pressure conditions attained in this method may point out the direction of a synthesis route for ionic orthocarbonates. On the other hand, no evidence for coordination changes or polymerization of NO_4^{3-} groups was found during the investigation of Na_3NO_4 at high pressure and ambient temperature. Broadening or vanishing of Raman and X-ray diffraction peaks corresponding to Na_2O and $NaNO_3$ above 13 GPa suggest pressure-induced amorphization or metastable phase transitions of the precursor mixture.

Acknowledgements

This work was supported by an EPSRC Senior Research Fellowship (grant number EP/D0735X) to PFM. We thank Alistair Lennie (now at Diamond Light Source, UK) for his support during diamond cell synchrotron runs at 9.5 HPHT, SRS and the Swiss-Norwegian Beam Lines (BM01A) for allowing us to run the XRD pattern of the sample at ambient conditions.

References

[1] R.J. Hemley (Ed.), Ultrahigh-Pressure Mineralogy, Vol. 37 of Reviews in Mineralogy, Mineralogical Society of America, 1998
[2] Stebbins J. F., McMillan P. F. and Dingwell D. B. (Eds), Structure, Dynamics and Properties of Silicate Melts, Vol. 32 of Reviews in Mineralogy;, Mineralogical Society of America, 1995; X. Xue, M. Kanzaki, R.G. Tronnes, J.F. Stebbins, Science 245 (1989) 962-964.
[3] D.J. Durben, P.F. McMillan, G.H. Wolf, Am. Mineral. 78 (1993) 1143-1148.
[4] R.A. Brooker, S.C. Kohn, J.R. Holloway, P.F. McMillan, M.R. Carroll, Geochim. Cosmochim. Acta 63 (1999) 3549-3565.
[5] M. Jansen, Z. Anorg. Allg. Chem. 491 (1982) 175-183.
[6] M. Jansen, Angew. Chem. Int. Ed. Engl. 16 (1977) 534-535.
[7] M. Jansen, Angew. Chem. Int. Ed. Engl. 18 (1977) 698-699.
[8] M. Al-Shemali, A.I. Boldyrev, J. Phys. Chem. A 106 (2002) 8951-8954.
[9] Z. Cancarevic, J.C. Schön, M. Jansen, Z. Anorg. Allg. Chem. 632 (2006) 2084.
[10] Z.P. Cancarevic, J.C. Schön, M. Jansen, Chem. Eur. J. 13 (2007) 7330-7348.
[11] V. Iota, C.S. Yoo, H. Cynn, Science 283 (1999) 1510-1513; M. Santoro, J-f. Lin, H-k. Mao, R.J. Hemley, J. Chem. Phys. 121 (2004) 2780-2787; O. Tschauner, H-k. Mao, R.J. Hemley, Phys. Rev. Lett. 87 (2001) 075701/01-075701/04.
[12] A.R. Oganov, C.W. Glass, S. Ono, Earth Planet. Sci. Lett. 241 (2006) 95-103.
[13] M. Santoro, F.A. Gorelli, R. Bini, G. Ruocco, S. Scandolo, W.A. Crichton, Nature 441 (2006) 857-860.
[14] A.C. Hess, P.F. McMillan, M. O'Keeffe, J. Phys. Chem. 92 (1988) 1785-1791.
[15] R.A. Forman, G.J. Piermarini, J.D. Barnett, S. Block, Science, New Series 176 (1972) 284-285.
[16] E. Soignard, P.F. McMillan, Chem. Mater. 16 (2004) 3533-3542.
[17] G.N. Greaves, C.R.A. Catlow, G.E. Derbyshire, M.I. McMahon, R.J. Nelmes, G. van der Laan, Nature Mat. 7 (2008) 827-830.
[18] A.R. Lennie, D. Laundy, M.A. Roberts, G. Bushnell-Wye, J. Synchrotron Rad. 14 (2007) 433-438.
[19] A.P. Hammersley, S.O. Svensson, M. Hanfland, A.N. Fitch, D. Häusermann, High Pressure Res. 14 (1996) 235-248.
[20] J. Rodriguez-Carvajal, FULLPROF suite, LLB Saclay and LCSIM Rennes, France, 2003.
[21] D. Walker, M.A. Carpenter, C.M. Hitch, Am. Mineral. 75 (1990) 1020-1028.
[22] H. Liu, W. Klein, A. Sani, M. Jansen, Phys. Chem. Chem. Phys. 6 (2004) 881-883.
[23] Y. Song, M. Somayazulu, H-k. Mao, R.J. Hemley, D.R. Herschbach, J. Chem. Phys.

118 (2003) 8350-8356.
[24] A. Lazicki, C.-S. Yoo, W.J. Evans, W.E. Pickett, Phys. Rev. B 73 (2006) 184120-1/-7; K. Kunc, I. Loa, A. Grzechnik, K. Sysassen, Phys. Stat. Solidi B 242 (2005) 1857-1863.

Figures

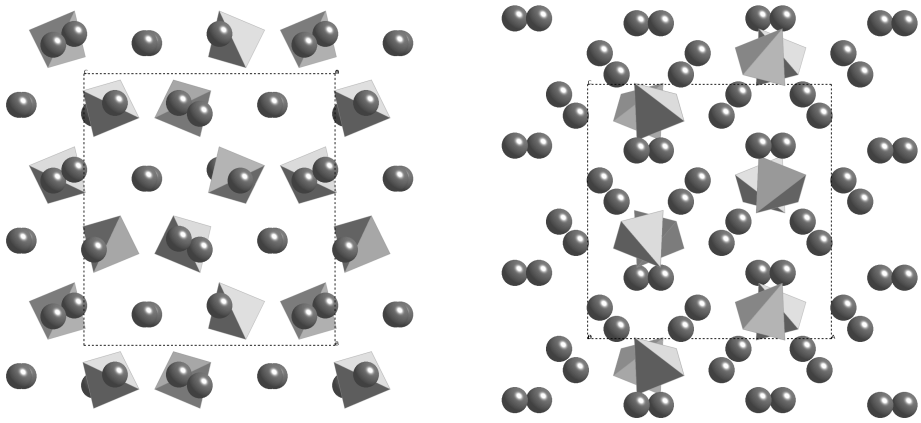

Fig. 1. Two views of the orthorhombic (*Pbca*) Na_3NO_4 structure reported in ref. [3] at ambient conditions. View along *a* (left) and *b* axes (right). The NO_4^{3-} groups are indicated by filled tetrahedra surrounded by Na^+ ions (circles).

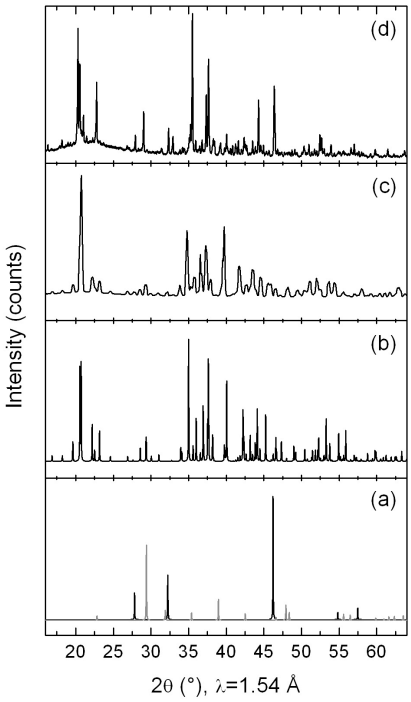

Fig. 2 – Powder X-ray diffraction patterns at ambient P,T conditions from (a) mixture of Na_2O (black) and $NaNO_3$ (grey) used as precursors (b) calculated Na_3NO_4 from ref. [3] (c) pure Na_3NO_4 found after synthesis at 380°C/90 days at room pressure, (d) Na_3NO_4 after synthesis in the multianvil cell at 4 GPa/500°C/2 days. The pattern shown in (c) was obtained using λ= 0.7 Å at BM01A, the Swiss-Norwegian Beam Lines (ESRF) but with 2θ values re-calculated for Cu$K\alpha_1$ radiation for comparison with other patterns.

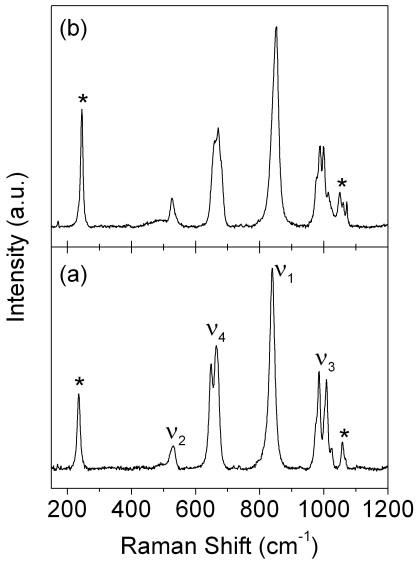

Fig. 3 - Raman spectra of Na_3NO_4 at ambient conditions after synthesis at (a) 380°C/90 days at room pressure and (b) 4 GPa/500°C/2 days. The corresponding vibrational modes are indicated [3]; the additional features are due to unreacted Na_2O and $NaNO_3$ (symbols).

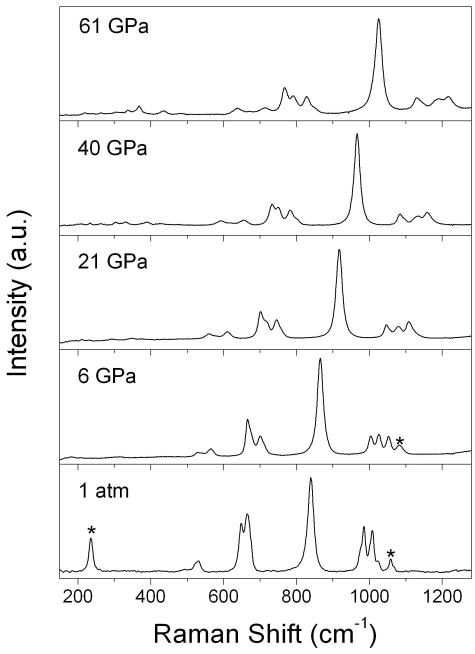

Fig. 4 - Raman spectra of Na_3NO_4 during compression at room temperature. We typically avoided those regions contaminated with any precursor in this study, but illustrate in some spectra the presence of Na_2O and $NaNO_3$ in the sample (symbols).

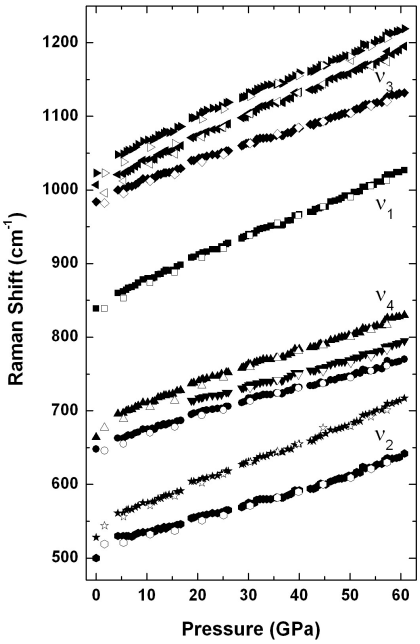

Fig. 5 - Raman shifts of Na_3NO_4 during compression (full circles) and decompression (empty circles) runs. All pressure-induced changes were found to be fully reversible.

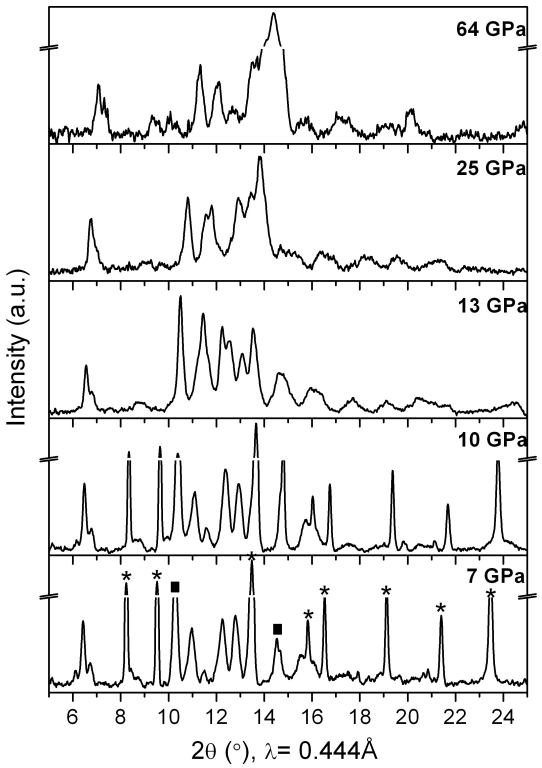

Fig. 6. Powder X-ray diffraction patterns from Na_3NO_4 upon pressurization under non-hydrostatic conditions. The symbols mark reflections corresponding to $NaNO_3$ (■) and Na_2O (*).

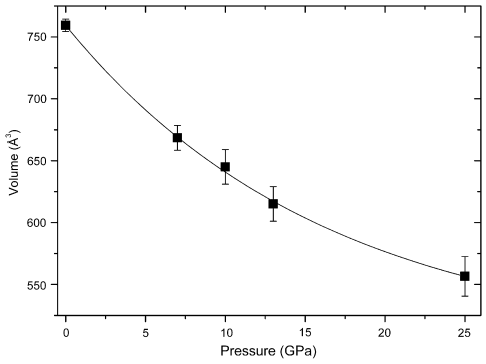

Fig. 7. Volume reduction upon compression up to 25 GPa. A bulk modulus of 43 ± 3 GPa^{-1} was estimated from this curve using a third order Birch-Murnaghan fit to the data (assuming $K_0' = 4$).

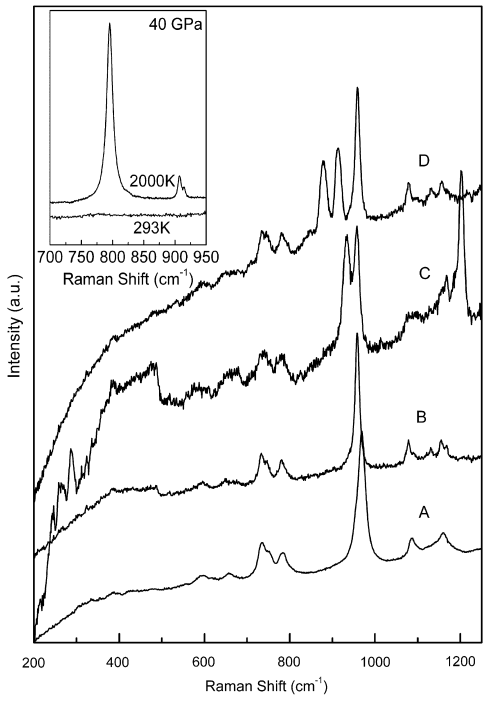

Fig. 7. Raman patterns of Na_3NO_4 before (A) and after laser heating (B,C,D) at ~36 GPa. The inset illustrates the transformation from CO_2-III (bottom) to CO_2-V (top) at 40 GPa and ~2000K observed in our laboratory. The laser heating experiment on Na_3NO_4 was carried out using similar conditions. In the polymerised CO_2-V structure the strong band at 790 cm^{-1} corresponds to the characteristic intertetrahedral C-O-C stretching mode.

Table 1. Bulk moduli of Na_3NO_4 and related materials. The corresponding values for Na_2O are also compared to other cubic antifluorite-structured compounds. K_0' other than 4 are indicated.

Table 1

	Bulk modulus (K_0), GPa	
	Experimental	*Calculated*
Na_3NO_4	43[a]	
Na_3ONO_2	47[b]	
$NO^+NO_3^-$	45.2[c]	
$NaNO_2$	21.9[d]	
$NaNO_3$	25.8[d]	
Li_4CO_4-IV	–	45.8[e]
Na_2O	83[a]	57.5-62.1[f]
	88[a] (K_0'=3.51)	
	74[a] (K_0' = 5.2)	
Li_2O	90[g] (K_0'=3.51)	94.6-105[f]
	75[g] (K_0' = 5.2)	
K_2O	–	33.4-40.7[f]
Rb_2O	–	30-35.8[f]

[a]This work.
[b]Ref.[17].
[c]Ref.[18].
[d]Ref.[19].
[e]Ref.[8].
[f]Ref. [21].
[g]Ref.[20].